

Welcome to [E-XFL.COM](https://www.e-xfl.com)

Understanding **Embedded - FPGAs (Field Programmable Gate Array)**

Embedded - FPGAs, or Field Programmable Gate Arrays, are advanced integrated circuits that offer unparalleled flexibility and performance for digital systems. Unlike traditional fixed-function logic devices, FPGAs can be programmed and reprogrammed to execute a wide array of logical operations, enabling customized functionality tailored to specific applications. This reprogrammability allows developers to iterate designs quickly and implement complex functions without the need for custom hardware.

Applications of Embedded - FPGAs

The versatility of Embedded - FPGAs makes them indispensable in numerous fields. In telecommunications.

Details

| | |
|--------------------------------|---|
| Product Status | Active |
| Number of LABs/CLBs | - |
| Number of Logic Elements/Cells | - |
| Total RAM Bits | 110592 |
| Number of I/O | 119 |
| Number of Gates | 600000 |
| Voltage - Supply | 1.425V ~ 1.575V |
| Mounting Type | Surface Mount |
| Operating Temperature | 0°C ~ 85°C (TJ) |
| Package / Case | 256-LBGA |
| Supplier Device Package | 256-FPBGA (17x17) |
| Purchase URL | https://www.e-xfl.com/product-detail/microchip-technology/afs600-fg256 |

Routing Architecture

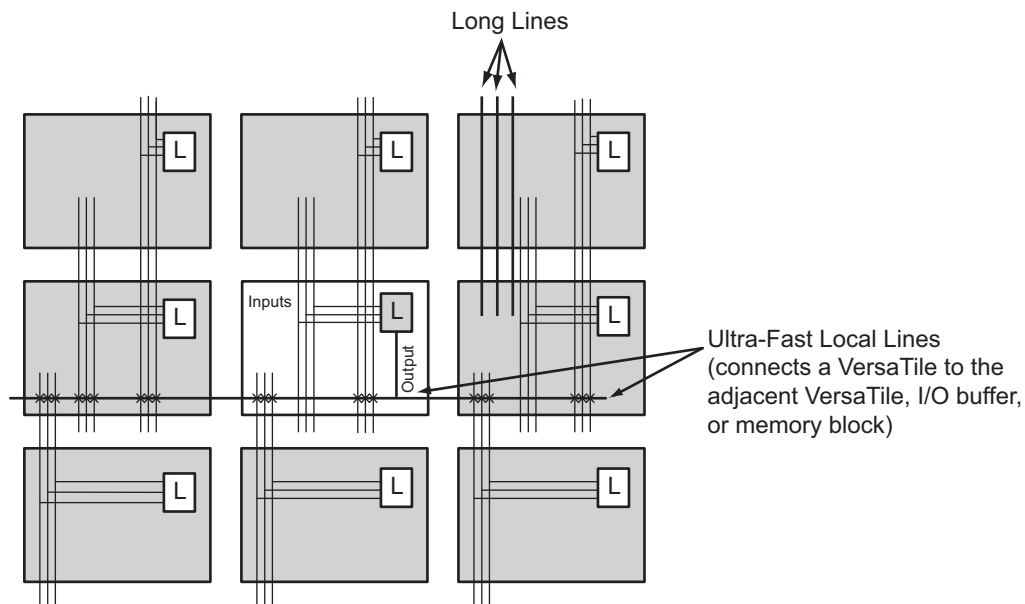
The routing structure of Fusion devices is designed to provide high performance through a flexible four-level hierarchy of routing resources: ultra-fast local resources; efficient long-line resources; high-speed very-long-line resources; and the high-performance VersaNet networks.

The ultra-fast local resources are dedicated lines that allow the output of each VersaTile to connect directly to every input of the eight surrounding VersaTiles (Figure 2-8). The exception to this is that the SET/CLR input of a VersaTile configured as a D-flip-flop is driven only by the VersaNet global network.

The efficient long-line resources provide routing for longer distances and higher-fanout connections. These resources vary in length (spanning one, two, or four VersaTiles), run both vertically and horizontally, and cover the entire Fusion device (Figure 2-9 on page 2-9). Each VersaTile can drive signals onto the efficient long-line resources, which can access every input of every VersaTile. Active buffers are inserted automatically by routing software to limit loading effects.

The high-speed very-long-line resources, which span the entire device with minimal delay, are used to route very long or high-fanout nets: length ± 12 VersaTiles in the vertical direction and length ± 16 in the horizontal direction from a given core VersaTile (Figure 2-10 on page 2-10). Very long lines in Fusion devices, like those in ProASIC3 devices, have been enhanced. This provides a significant performance boost for long-reach signals.

The high-performance VersaNet global networks are low-skew, high-fanout nets that are accessible from external pins or from internal logic (Figure 2-11 on page 2-11). These nets are typically used to distribute clocks, reset signals, and other high-fanout nets requiring minimum skew. The VersaNet networks are implemented as clock trees, and signals can be introduced at any junction. These can be employed hierarchically, with signals accessing every input on all VersaTiles.



Note: Input to the core cell for the D-flip-flop set and reset is only available via the VersaNet global network connection.

Figure 2-8 • Ultra-Fast Local Lines Connected to the Eight Nearest Neighbors

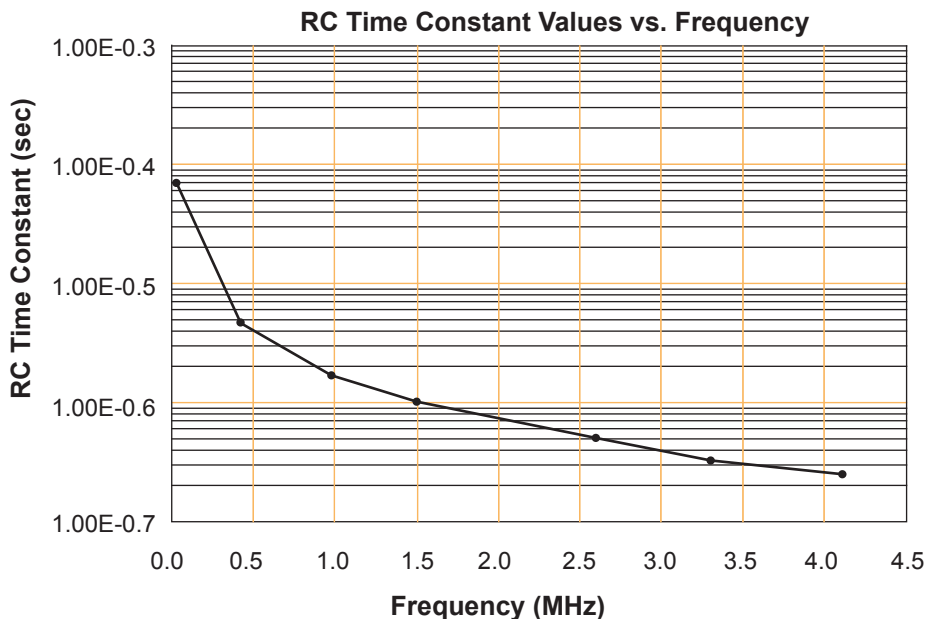


Figure 2-18 • Crystal Oscillator: RC Time Constant Values vs. Frequency (typical)

Table 2-10 • XTLOSC Signals Descriptions

| Signal Name | Width | Direction | Function | | |
|---------------|-------|-----------|---|---|-----------------|
| XTL_EN* | 1 | | Enables the crystal. Active high. | | |
| XTL_MODE* | 2 | | Settings for the crystal clock for different frequency. | | |
| | | | Value | Modes | Frequency Range |
| | | | b'00 | RC network | 32 KHz to 4 MHz |
| | | | b'01 | Low gain | 32 to 200 KHz |
| | | | b'10 | Medium gain | 0.20 to 2.0 MHz |
| | | | b'11 | High gain | 2.0 to 20.0 MHz |
| SELMODE | 1 | IN | Selects the source of XTL_MODE and also enables the XTL_EN. Connect from RTCXTLSEL from AB. | | |
| | | | 0 | For normal operation or sleep mode, XTL_EN depends on FPGA_EN, XTL_MODE depends on MODE | |
| | | | 1 | For Standby mode, XTL_EN is enabled, XTL_MODE depends on RTC_MODE | |
| RTC_MODE[1:0] | 2 | IN | Settings for the crystal clock for different frequency ranges. XTL_MODE uses RTC_MODE when SELMODE is '1'. | | |
| MODE[1:0] | 2 | IN | Settings for the crystal clock for different frequency ranges. XTL_MODE uses MODE when SELMODE is '0'. In Standby, MODE inputs will be 0's. | | |
| FPGA_EN* | 1 | IN | 0 when 1.5 V is not present for VCC 1 when 1.5 V is present for VCC | | |
| XTL | 1 | IN | Crystal Clock source | | |
| CLKOUT | 1 | OUT | Crystal Clock output | | |

Note: *Internal signal—does not exist in macro.

Clock Conditioning Circuits

In Fusion devices, the CCCs are used to implement frequency division, frequency multiplication, phase shifting, and delay operations.

The CCCs are available in six chip locations—each of the four chip corners and the middle of the east and west chip sides.

Each CCC can implement up to three independent global buffers (with or without programmable delay), or a PLL function (programmable frequency division/multiplication, phase shift, and delays) with up to three global outputs. Unused global outputs of a PLL can be used to implement independent global buffers, up to a maximum of three global outputs for a given CCC.

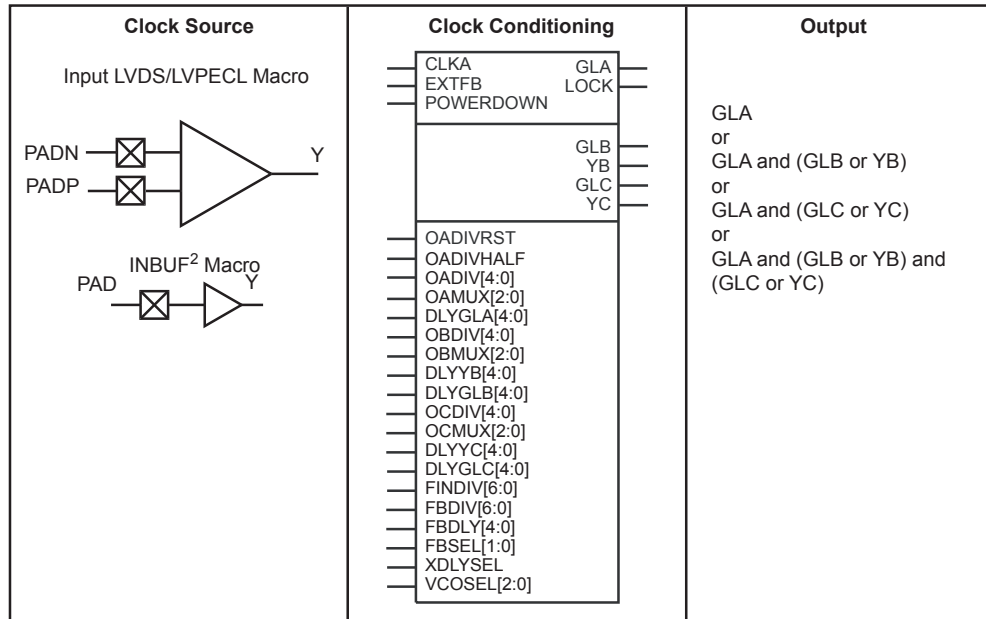
A global buffer can be placed in any of the three global locations (CLKA-GLA, CLKB-GLB, and CLKC-GLC) of a given CCC.

A PLL macro uses the CLKA CCC input to drive its reference clock. It uses the GLA and, optionally, the GLB and GLC global outputs to drive the global networks. A PLL macro can also drive the YB and YC regular core outputs. The GLB (or GLC) global output cannot be reused if the YB (or YC) output is used (Figure 2-19). Refer to the "PLL Macro" section on page 2-27 for more information.

Each global buffer, as well as the PLL reference clock, can be driven from one of the following:

- 3 dedicated single-ended I/Os using a hardwired connection
- 2 dedicated differential I/Os using a hardwired connection
- The FPGA core

The CCC block is fully configurable, either via flash configuration bits set in the programming bitstream or through an asynchronous interface. This asynchronous interface is dynamically accessible from inside the Fusion device to permit changes of parameters (such as divide ratios) during device operation. To increase the versatility and flexibility of the clock conditioning system, the CCC configuration is determined either by the user during the design process, with configuration data being stored in flash memory as part of the device programming procedure, or by writing data into a dedicated shift register during normal device operation. This latter mode allows the user to dynamically reconfigure the CCC without the need for core programming. The shift register is accessed through a simple serial interface. Refer to the "UJTAG Applications in Microsemi's Low-Power Flash Devices" chapter of the *Fusion FPGA Fabric User Guide* and the "CCC and PLL Characteristics" section on page 2-28 for more information.



Notes:

1. Visit the [Microsemi SoC Products Group website](#) for application notes concerning dynamic PLL reconfiguration. Refer to the "PLL Macro" section on page 2-27 for signal descriptions.
2. Many specific INBUF macros support the wide variety of single-ended and differential I/O standards for the Fusion family.
3. Refer to the [IGLOO](#), [ProASIC3](#), [SmartFusion](#) and [Fusion Macro Library Guide](#) for more information.

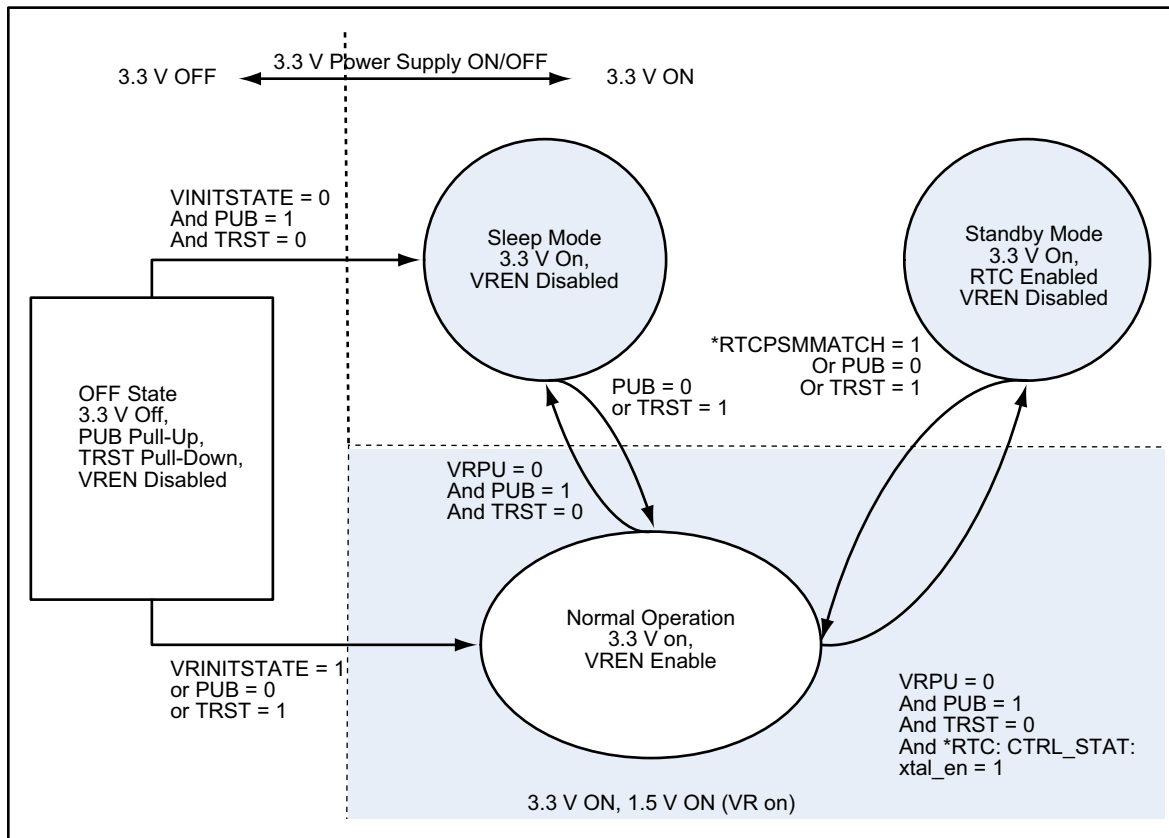
Figure 2-19 • Fusion CCC Options: Global Buffers with the PLL Macro

Table 2-11 • Available Selections of I/O Standards within CLKBUF and CLKBUF_LVDS/LVPECL Macros

| CLKBUF Macros |
|------------------------------|
| CLKBUF_LVCMOS5 |
| CLKBUF_LVCMOS33 ¹ |
| CLKBUF_LVCMOS18 |
| CLKBUF_LVCMOS15 |
| CLKBUF_PCI |
| CLKBUF_LVDS ² |
| CLKBUF_LVPECL |

Notes:

1. This is the default macro. For more details, refer to the [IGLOO](#), [ProASIC3](#), [SmartFusion](#) and [Fusion Macro Library Guide](#).
2. The B-LVDS and M-LVDS standards are supported with CLKBUF_LVDS.



Note: * To enter and exit standby mode without any external stimulus on PUB or TRST, the `vr_en_mat` in the `CTRL_STAT` register must also be set to 1, so that `RTCPSMMATCH` will assert when a match occurs; hence the device exits standby mode.

Figure 2-31 • State Diagram for All Different Power Modes

When TRST is 1 or PUB is 0, the 1.5 V voltage regulator is always ON, putting the Fusion device in normal operation at all times. Therefore, when the JTAG port is not in reset, the Fusion device cannot enter sleep mode or standby mode.

To enter standby mode, the Fusion device must first power-up into normal operation. The RTC is enabled through the RTC Control/Status Register described in the ["Real-Time Counter \(part of AB macro\)" section on page 2-33](#). A match value corresponding to the wake-up time is loaded into the Match Register. The 1.5 V voltage regulator is disabled by setting VRPU to 0 to allow the Fusion device to enter standby mode, when the 1.5 V supply is off but the RTC remains on.

The following signals are used to configure the RAM4K9 memory element.

WIDTHA and WIDTHB

These signals enable the RAM to be configured in one of four allowable aspect ratios (Table 2-27).

Table 2-27 • Allowable Aspect Ratio Settings for WIDTHA[1:0]

| WIDTHA1, WIDTHA0 | WIDTHB1, WIDTHB0 | D×W |
|------------------|------------------|-------|
| 00 | 00 | 4k×1 |
| 01 | 01 | 2k×2 |
| 10 | 10 | 1k×4 |
| 11 | 11 | 512×9 |

Note: The aspect ratio settings are constant and cannot be changed on the fly.

BLKA and BLKB

These signals are active low and will enable the respective ports when asserted. When a BLKx signal is deasserted, the corresponding port's outputs hold the previous value.

WENA and WENB

These signals switch the RAM between read and write mode for the respective ports. A Low on these signals indicates a write operation, and a High indicates a read.

CLKA and CLKB

These are the clock signals for the synchronous read and write operations. These can be driven independently or with the same driver.

PIPEA and PIPEB

These signals are used to specify pipelined read on the output. A Low on PIPEA or PIPEB indicates a nonpipelined read, and the data appears on the corresponding output in the same clock cycle. A High indicates a pipelined, read and data appears on the corresponding output in the next clock cycle.

WMODEA and WMODEB

These signals are used to configure the behavior of the output when the RAM is in write mode. A Low on these signals makes the output retain data from the previous read. A High indicates pass-through behavior, wherein the data being written will appear immediately on the output. This signal is overridden when the RAM is being read.

RESET

This active low signal resets the output to zero, disables reads and writes from the SRAM block, and clears the data hold registers when asserted. It does not reset the contents of the memory.

ADDRA and ADDRb

These are used as read or write addresses, and they are 12 bits wide. When a depth of less than 4 k is specified, the unused high-order bits must be grounded (Table 2-28).

Table 2-28 • Address Pins Unused/Used for Various Supported Bus Widths

| D×W | ADDRx | |
|-------|---------|--------|
| | Unused | Used |
| 4k×1 | None | [11:0] |
| 2k×2 | [11] | [10:0] |
| 1k×4 | [11:10] | [9:0] |
| 512×9 | [11:9] | [8:0] |

Note: The "x" in ADDR_x implies A or B.

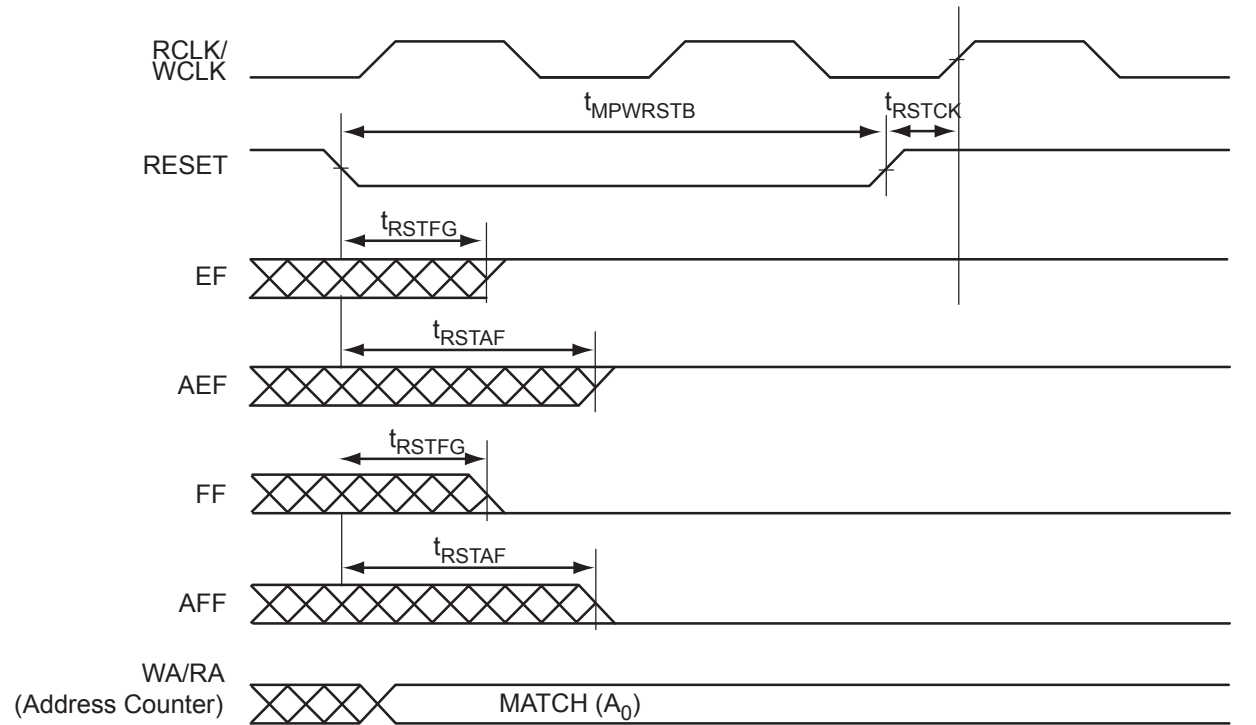


Figure 2-59 • FIFO Reset

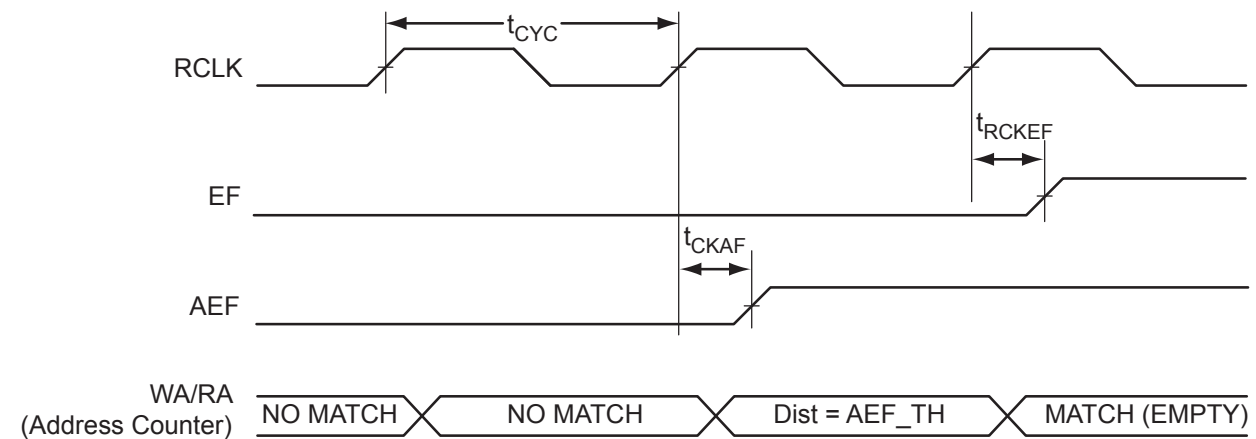


Figure 2-60 • FIFO EMPTY Flag and AEMPTY Flag Assertion

Analog Block

With the Fusion family, Microsemi has introduced the world's first mixed-mode FPGA solution. Supporting a robust analog peripheral mix, Fusion devices will support a wide variety of applications. It is this Analog Block that separates Fusion from all other FPGA solutions on the market today.

By combining both flash and high-speed CMOS processes in a single chip, these devices offer the best of both worlds. The high-performance CMOS is used for building RAM resources. These high-performance structures support device operation up to 350 MHz. Additionally, the advanced Microsemi 0.13 μm flash process incorporates high-voltage transistors and a high-isolation, triple-well process. Both of these are suited for the flash-based programmable logic and nonvolatile memory structures.

High-voltage transistors support the integration of analog technology in several ways. They aid in noise immunity so that the analog portions of the chip can be better isolated from the digital portions, increasing analog accuracy. Because they support high voltages, Microsemi flash FPGAs can be connected directly to high-voltage input signals, eliminating the need for external resistor divider networks, reducing component count, and increasing accuracy. By supporting higher internal voltages, the Microsemi advanced flash process enables high dynamic range on analog circuitry, increasing precision and signal-noise ratio. Microsemi flash FPGAs also drive high-voltage outputs, eliminating the need for external level shifters and drivers.

The unique triple-well process enables the integration of high-performance analog features with increased noise immunity and better isolation. By increasing the efficiency of analog design, the triple-well process also enables a smaller overall design size, reducing die size and cost.

The Analog Block consists of the Analog Quad I/O structure, RTC (for details refer to the "[Real-Time Counter System](#)" section on page 2-31), ADC, and ACM. All of these elements are combined in the single Analog Block macro, with which the user implements this functionality ([Figure 2-64](#)).

The Analog Block needs to be reset/reinitialized after the core powers up or the device is programmed. An external reset/initialize signal, which can come from the internal voltage regulator when it powers up, must be applied.

This process results in a binary approximation of VIN. Generally, there is a fixed interval T, the sampling period, between the samples. The inverse of the sampling period is often referred to as the sampling frequency $f_s = 1 / T$. The combined effect is illustrated in [Figure 2-82](#).

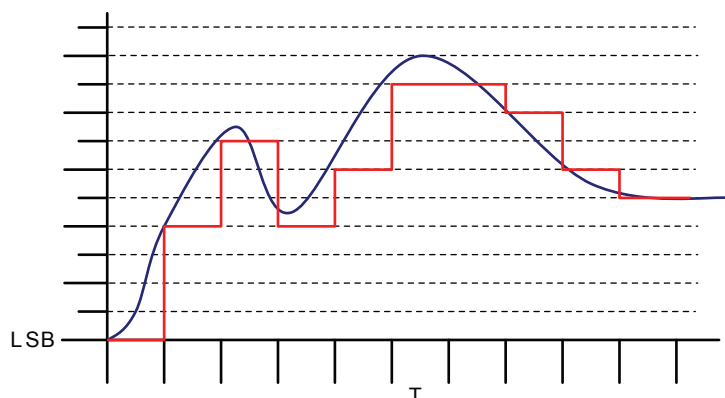


Figure 2-82 • Conversion Example

[Figure 2-82](#) demonstrates that if the signal changes faster than the sampling rate can accommodate, or if the actual value of VIN falls between counts in the result, this information is lost during the conversion. There are several techniques that can be used to address these issues.

First, the sampling rate must be chosen to provide enough samples to adequately represent the input signal. Based on the Nyquist-Shannon Sampling Theorem, the minimum sampling rate must be at least twice the frequency of the highest frequency component in the target signal (Nyquist Frequency). For example, to recreate the frequency content of an audio signal with up to 22 KHz bandwidth, the user must sample it at a minimum of 44 ksps. However, as shown in [Figure 2-82](#), significant post-processing of the data is required to interpolate the value of the waveform during the time between each sample.

Similarly, to re-create the amplitude variation of a signal, the signal must be sampled with adequate resolution. Continuing with the audio example, the dynamic range of the human ear (the ratio of the amplitude of the threshold of hearing to the threshold of pain) is generally accepted to be 135 dB, and the dynamic range of a typical symphony orchestra performance is around 85 dB. Most commercial recording media provide about 96 dB of dynamic range using 16-bit sample resolution. But 16-bit fidelity does not necessarily mean that you need a 16-bit ADC. As long as the input is sampled at or above the Nyquist Frequency, post-processing techniques can be used to interpolate intermediate values and reconstruct the original input signal to within desired tolerances.

If sophisticated digital signal processing (DSP) capabilities are available, the best results are obtained by implementing a reconstruction filter, which is used to interpolate many intermediate values with higher resolution than the original data. Interpolating many intermediate values increases the effective number of samples, and higher resolution increases the effective number of bits in the sample. In many cases, however, it is not cost-effective or necessary to implement such a sophisticated reconstruction algorithm. For applications that do not require extremely fine reproduction of the input signal, alternative methods can enhance digital sampling results with relatively simple post-processing. The details of such techniques are out of the scope of this chapter; refer to the [Improving ADC Results through Oversampling and Post-Processing of Data](#) white paper for more information.

ADC Terminology

Conversion Time

Conversion time is the interval between the release of the hold state (imposed by the input circuitry of a track-and-hold) and the instant at which the voltage on the sampling capacitor settles to within one LSB of a new input value.

DNL – Differential Non-Linearity

For an ideal ADC, the analog-input levels that trigger any two successive output codes should differ by one LSB (DNL = 0). Any deviation from one LSB is defined as DNL (Figure 2-83).



Figure 2-83 • Differential Non-Linearity (DNL)

ENOB – Effective Number of Bits

ENOB specifies the dynamic performance of an ADC at a specific input frequency and sampling rate. An ideal ADC's error consists only of quantization of noise. As the input frequency increases, the overall noise (particularly in the distortion components) also increases, thereby reducing the ENOB and SINAD (also see "Signal-to-Noise and Distortion Ratio (SINAD)".) ENOB for a full-scale, sinusoidal input waveform is computed using EQ 12.

$$ENOB = \frac{SINAD - 1.76}{6.02}$$

EQ 12

FS Error – Full-Scale Error

Full-scale error is the difference between the actual value that triggers that transition to full-scale and the ideal analog full-scale transition value. Full-scale error equals offset error plus gain error.

Solution 3

The board-level design must ensure that the reflected waveform at the pad does not exceed limits provided in Table 3-4 on page 3-4. This is a long-term reliability requirement.

This scheme will also work for a 3.3 V PCI/PCIX configuration, but the internal diode should not be used for clamping, and the voltage must be limited by the bus switch, as shown in Figure 2-105. Relying on the diode clamping would create an excessive pad DC voltage of $3.3\text{ V} + 0.7\text{ V} = 4\text{ V}$.

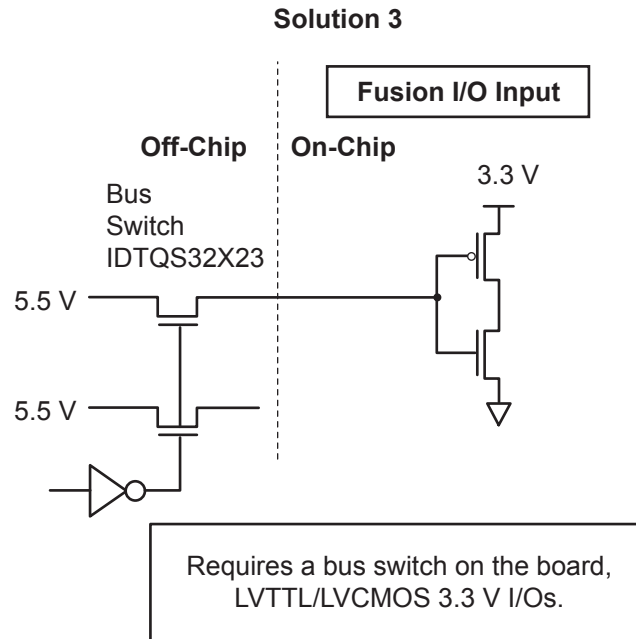


Figure 2-105 • Solution 3

Solution 4

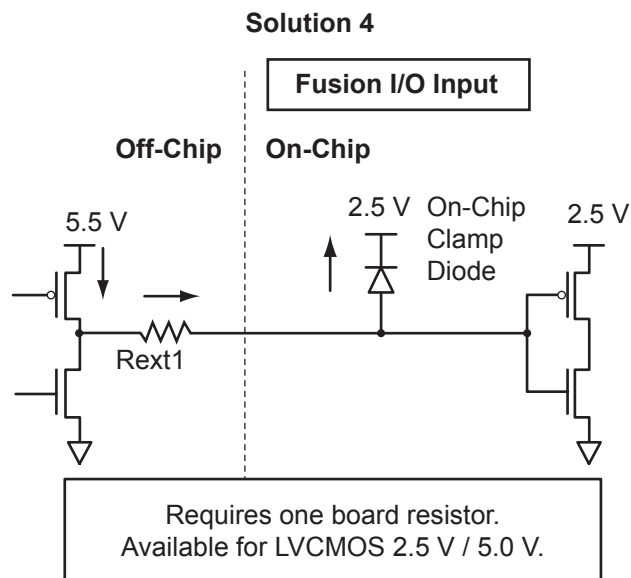


Figure 2-106 • Solution 4

User I/O Naming Convention

Due to the comprehensive and flexible nature of Fusion device user I/Os, a naming scheme is used to show the details of the I/O (Figure 2-113 on page 2-158 and Figure 2-114 on page 2-159). The name identifies to which I/O bank it belongs, as well as the pairing and pin polarity for differential I/Os.

I/O Nomenclature = Gmn/IOuxwByVz

Gmn is only used for I/Os that also have CCC access—i.e., global pins.

G = Global

m = Global pin location associated with each CCC on the device: A (northwest corner), B (northeast corner), C (east middle), D (southeast corner), E (southwest corner), and F (west middle).

n = Global input MUX and pin number of the associated Global location m, either A0, A1, A2, B0, B1, B2, C0, C1, or C2. Figure 2-22 on page 2-25 shows the three input pins per clock source MUX at CCC location m.

u = I/O pair number in the bank, starting at 00 from the northwest I/O bank and proceeding in a clockwise direction.

x = P (Positive) or N (Negative) for differential pairs, or R (Regular – single-ended) for the I/Os that support single-ended and voltage-referenced I/O standards only. U (Positive-LVDS only) or V (Negative-LVDS only) restrict the I/O differential pair from being selected as an LVPECL pair.

w = D (Differential Pair), P (Pair), or S (Single-Ended). D (Differential Pair) if both members of the pair are bonded out to adjacent pins or are separated only by one GND or NC pin; P (Pair) if both members of the pair are bonded out but do not meet the adjacency requirement; or S (Single-Ended) if the I/O pair is not bonded out. For Differential (D) pairs, adjacency for ball grid packages means only vertical or horizontal. Diagonal adjacency does not meet the requirements for a true differential pair.

B = Bank

y = Bank number (0–3). The Bank number starts at 0 from the northwest I/O bank and proceeds in a clockwise direction.

V = Reference voltage

z = Minibank number

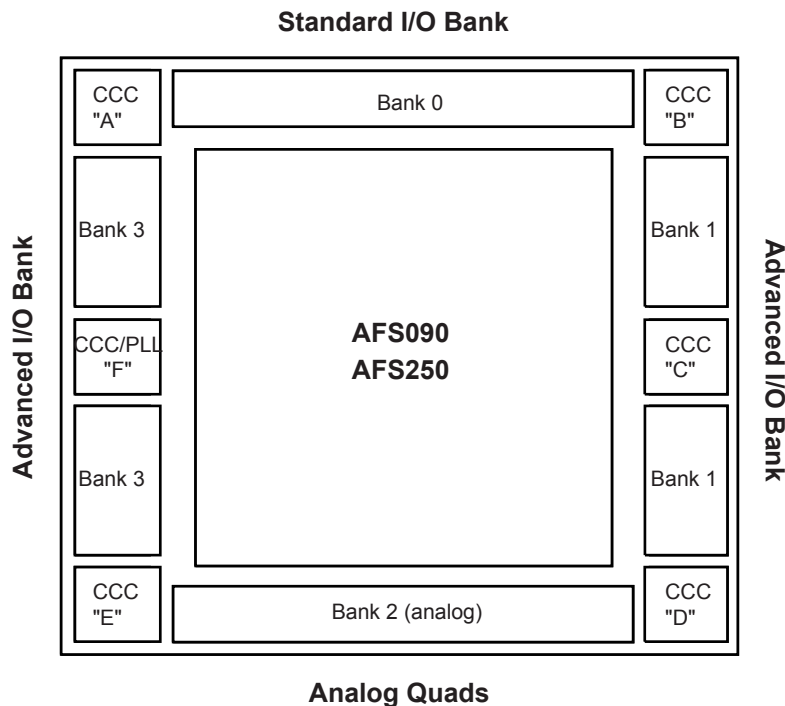


Figure 2-113 • Naming Conventions of Fusion Devices with Three Digital I/O Banks

Table 2-107 • 3.3 V LVTTTL / 3.3 V LVCMOS High Slew
Commercial Temperature Range Conditions: $T_J = 70^\circ\text{C}$, Worst-Case $V_{CC} = 1.425\text{ V}$,
Worst-Case $V_{CCI} = 3.0\text{ V}$
Applicable to Advanced I/Os

| Drive Strength | Speed Grade | t_{DOUT} | t_{DP} | t_{DIN} | t_{PY} | t_{EOUT} | t_{ZL} | t_{ZH} | t_{LZ} | t_{HZ} | t_{ZLS} | t_{ZHS} | Units |
|----------------|-------------|------------|----------|-----------|----------|------------|----------|----------|----------|----------|-----------|-----------|-------|
| 4 mA | Std. | 0.66 | 7.66 | 0.04 | 1.20 | 0.43 | 7.80 | 6.59 | 2.65 | 2.61 | 10.03 | 8.82 | ns |
| | -1 | 0.56 | 6.51 | 0.04 | 1.02 | 0.36 | 6.63 | 5.60 | 2.25 | 2.22 | 8.54 | 7.51 | ns |
| | -2 | 0.49 | 5.72 | 0.03 | 0.90 | 0.32 | 5.82 | 4.92 | 1.98 | 1.95 | 7.49 | 6.59 | ns |
| 8 mA | Std. | 0.66 | 4.91 | 0.04 | 1.20 | 0.43 | 5.00 | 4.07 | 2.99 | 3.20 | 7.23 | 6.31 | ns |
| | -1 | 0.56 | 4.17 | 0.04 | 1.02 | 0.36 | 4.25 | 3.46 | 2.54 | 2.73 | 6.15 | 5.36 | ns |
| | -2 | 0.49 | 3.66 | 0.03 | 0.90 | 0.32 | 3.73 | 3.04 | 2.23 | 2.39 | 5.40 | 4.71 | ns |
| 12 mA | Std. | 0.66 | 3.53 | 0.04 | 1.20 | 0.43 | 3.60 | 2.82 | 3.21 | 3.58 | 5.83 | 5.06 | ns |
| | -1 | 0.56 | 3.00 | 0.04 | 1.02 | 0.36 | 3.06 | 2.40 | 2.73 | 3.05 | 4.96 | 4.30 | ns |
| | -2 | 0.49 | 2.64 | 0.03 | 0.90 | 0.32 | 2.69 | 2.11 | 2.40 | 2.68 | 4.36 | 3.78 | ns |
| 16 mA | Std. | 0.66 | 3.33 | 0.04 | 1.20 | 0.43 | 3.39 | 2.56 | 3.26 | 3.68 | 5.63 | 4.80 | ns |
| | -1 | 0.56 | 2.83 | 0.04 | 1.02 | 0.36 | 2.89 | 2.18 | 2.77 | 3.13 | 4.79 | 4.08 | ns |
| | -2 | 0.49 | 2.49 | 0.03 | 0.90 | 0.32 | 2.53 | 1.91 | 2.44 | 2.75 | 4.20 | 3.58 | ns |
| 24 mA | Std. | 0.66 | 3.08 | 0.04 | 1.20 | 0.43 | 3.13 | 2.12 | 3.32 | 4.06 | 5.37 | 4.35 | ns |
| | -1 | 0.56 | 2.62 | 0.04 | 1.02 | 0.36 | 2.66 | 1.80 | 2.83 | 3.45 | 4.57 | 3.70 | ns |
| | -2 | 0.49 | 2.30 | 0.03 | 0.90 | 0.32 | 2.34 | 1.58 | 2.48 | 3.03 | 4.01 | 3.25 | ns |

Note: For the derating values at specific junction temperature and voltage supply levels, refer to [Table 3-7 on page 3-9](#).

Table 2-108 • 3.3 V LVTTTL / 3.3 V LVCMOS Low Slew
Commercial Temperature Range Conditions: $T_J = 70^\circ\text{C}$, Worst-Case $V_{CC} = 1.425\text{ V}$,
Worst-Case $V_{CCI} = 3.0\text{ V}$
Applicable to Standard I/Os

| Drive Strength | Speed Grade | t_{DOUT} | t_{DP} | t_{DIN} | t_{PY} | t_{EOUT} | t_{ZL} | t_{ZH} | t_{LZ} | t_{HZ} | Units |
|----------------|-------------|------------|----------|-----------|----------|------------|----------|----------|----------|----------|-------|
| 2 mA | Std. | 0.66 | 9.46 | 0.04 | 1.00 | 0.43 | 9.64 | 8.54 | 2.07 | 2.04 | ns |
| | -1 | 0.56 | 8.05 | 0.04 | 0.85 | 0.36 | 8.20 | 7.27 | 1.76 | 1.73 | ns |
| | -2 | 0.49 | 7.07 | 0.03 | 0.75 | 0.32 | 7.20 | 6.38 | 1.55 | 1.52 | ns |
| 4 mA | Std. | 0.66 | 9.46 | 0.04 | 1.00 | 0.43 | 9.64 | 8.54 | 2.07 | 2.04 | ns |
| | -1 | 0.56 | 8.05 | 0.04 | 0.85 | 0.36 | 8.20 | 7.27 | 1.76 | 1.73 | ns |
| | -2 | 0.49 | 7.07 | 0.03 | 0.75 | 0.32 | 7.20 | 6.38 | 1.55 | 1.52 | ns |
| 6 mA | Std. | 0.66 | 6.57 | 0.04 | 1.00 | 0.43 | 6.69 | 5.98 | 2.40 | 2.57 | ns |
| | -1 | 0.56 | 5.59 | 0.04 | 0.85 | 0.36 | 5.69 | 5.09 | 2.04 | 2.19 | ns |
| | -2 | 0.49 | 4.91 | 0.03 | 0.75 | 0.32 | 5.00 | 4.47 | 1.79 | 1.92 | ns |
| 8 mA | Std. | 0.66 | 6.57 | 0.04 | 1.00 | 0.43 | 6.69 | 5.98 | 2.40 | 2.57 | ns |
| | -1 | 0.56 | 5.59 | 0.04 | 0.85 | 0.36 | 5.69 | 5.09 | 2.04 | 2.19 | ns |
| | -2 | 0.49 | 4.91 | 0.03 | 0.75 | 0.32 | 5.00 | 4.47 | 1.79 | 1.92 | ns |

Note: For the derating values at specific junction temperature and voltage supply levels, refer to [Table 3-7 on page 3-9](#).

$$P_{S-CELL} = N_{S-CELL} * (PAC5 + (\alpha_1 / 2) * PAC6) * F_{CLK}$$

N_{S-CELL} is the number of VersaTiles used as sequential modules in the design. When a multi-tile sequential cell is used, it should be accounted for as 1.

α_1 is the toggle rate of VersaTile outputs—guidelines are provided in [Table 3-16 on page 3-27](#).

F_{CLK} is the global clock signal frequency.

Standby Mode and Sleep Mode

$$P_{S-CELL} = 0 \text{ W}$$

Combinatorial Cells Dynamic Contribution— P_{C-CELL}

Operating Mode

$$P_{C-CELL} = N_{C-CELL} * (\alpha_1 / 2) * PAC7 * F_{CLK}$$

N_{C-CELL} is the number of VersaTiles used as combinatorial modules in the design.

α_1 is the toggle rate of VersaTile outputs—guidelines are provided in [Table 3-16 on page 3-27](#).

F_{CLK} is the global clock signal frequency.

Standby Mode and Sleep Mode

$$P_{C-CELL} = 0 \text{ W}$$

Routing Net Dynamic Contribution— P_{NET}

Operating Mode

$$P_{NET} = (N_{S-CELL} + N_{C-CELL}) * (\alpha_1 / 2) * PAC8 * F_{CLK}$$

N_{S-CELL} is the number VersaTiles used as sequential modules in the design.

N_{C-CELL} is the number of VersaTiles used as combinatorial modules in the design.

α_1 is the toggle rate of VersaTile outputs—guidelines are provided in [Table 3-16 on page 3-27](#).

F_{CLK} is the global clock signal frequency.

Standby Mode and Sleep Mode

$$P_{NET} = 0 \text{ W}$$

I/O Input Buffer Dynamic Contribution— P_{INPUTS}

Operating Mode

$$P_{INPUTS} = N_{INPUTS} * (\alpha_2 / 2) * PAC9 * F_{CLK}$$

N_{INPUTS} is the number of I/O input buffers used in the design.

α_2 is the I/O buffer toggle rate—guidelines are provided in [Table 3-16 on page 3-27](#).

F_{CLK} is the global clock signal frequency.

Standby Mode and Sleep Mode

$$P_{INPUTS} = 0 \text{ W}$$

I/O Output Buffer Dynamic Contribution— $P_{OUTPUTS}$

Operating Mode

$$P_{OUTPUTS} = N_{OUTPUTS} * (\alpha_2 / 2) * \beta_1 * PAC10 * F_{CLK}$$

$N_{OUTPUTS}$ is the number of I/O output buffers used in the design.

α_2 is the I/O buffer toggle rate—guidelines are provided in [Table 3-16 on page 3-27](#).

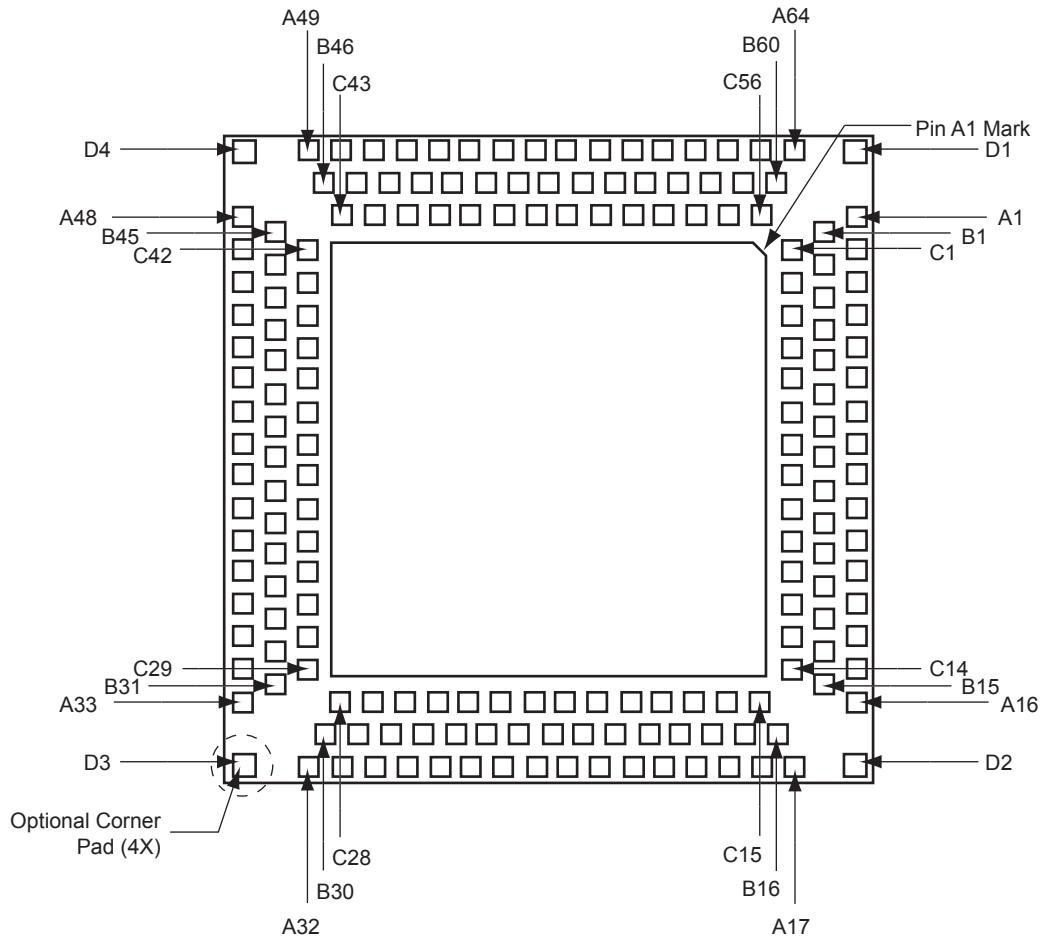
β_1 is the I/O buffer enable rate—guidelines are provided in [Table 3-17 on page 3-27](#).

F_{CLK} is the global clock signal frequency.

Standby Mode and Sleep Mode

$$P_{OUTPUTS} = 0 \text{ W}$$

QN180



Note: The die attach paddle center of the package is tied to ground (GND).

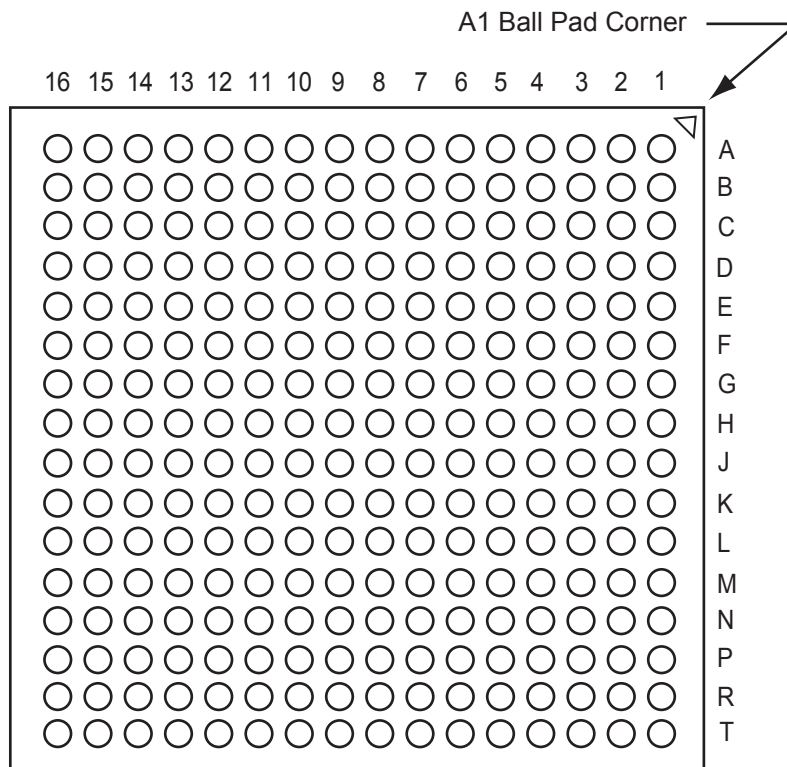
Note

For Package Manufacturing and Environmental information, visit the Resource Center at <http://www.microsemi.com/soc/products/solutions/package/default.aspx>.

| PQ208 | | |
|------------|-----------------|-----------------|
| Pin Number | AFS250 Function | AFS600 Function |
| 74 | AV2 | AV4 |
| 75 | AC2 | AC4 |
| 76 | AG2 | AG4 |
| 77 | AT2 | AT4 |
| 78 | ATR TN1 | ATR TN2 |
| 79 | AT3 | AT5 |
| 80 | AG3 | AG5 |
| 81 | AC3 | AC5 |
| 82 | AV3 | AV5 |
| 83 | AV4 | AV6 |
| 84 | AC4 | AC6 |
| 85 | AG4 | AG6 |
| 86 | AT4 | AT6 |
| 87 | ATR TN2 | ATR TN3 |
| 88 | AT5 | AT7 |
| 89 | AG5 | AG7 |
| 90 | AC5 | AC7 |
| 91 | AV5 | AV7 |
| 92 | NC | AV8 |
| 93 | NC | AC8 |
| 94 | NC | AG8 |
| 95 | NC | AT8 |
| 96 | NC | ATR TN4 |
| 97 | NC | AT9 |
| 98 | NC | AG9 |
| 99 | NC | AC9 |
| 100 | NC | AV9 |
| 101 | GND AQ | GND AQ |
| 102 | VCC33A | VCC33A |
| 103 | ADCGNDREF | ADCGNDREF |
| 104 | VAREF | VAREF |
| 105 | PUB | PUB |
| 106 | VCC33A | VCC33A |
| 107 | GND A | GND A |
| 108 | PTEM | PTEM |
| 109 | PTBASE | PTBASE |
| 110 | GND NVM | GND NVM |

| PQ208 | | |
|------------|-----------------|-----------------|
| Pin Number | AFS250 Function | AFS600 Function |
| 111 | VCCNVM | VCCNVM |
| 112 | VCC | VCC |
| 112 | VCC | VCC |
| 113 | VPUMP | VPUMP |
| 114 | GND Q | NC |
| 115 | VCCIB1 | TCK |
| 116 | TCK | TDI |
| 117 | TDI | TMS |
| 118 | TMS | TDO |
| 119 | TDO | TRST |
| 120 | TRST | VJTAG |
| 121 | VJTAG | IO57NDB2V0 |
| 122 | IO57NDB1V0 | GDC2/IO57PDB2V0 |
| 123 | GDC2/IO57PDB1V0 | IO56NDB2V0 |
| 124 | IO56NDB1V0 | GDB2/IO56PDB2V0 |
| 125 | GDB2/IO56PDB1V0 | IO55NDB2V0 |
| 126 | VCCIB1 | GDA2/IO55PDB2V0 |
| 127 | GND | GDA0/IO54NDB2V0 |
| 128 | IO55NDB1V0 | GDA1/IO54PDB2V0 |
| 129 | GDA2/IO55PDB1V0 | VCCIB2 |
| 130 | GDA0/IO54NDB1V0 | GND |
| 131 | GDA1/IO54PDB1V0 | VCC |
| 132 | GDB0/IO53NDB1V0 | GCA0/IO45NDB2V0 |
| 133 | GDB1/IO53PDB1V0 | GCA1/IO45PDB2V0 |
| 134 | GDC0/IO52NDB1V0 | GCB0/IO44NDB2V0 |
| 135 | GDC1/IO52PDB1V0 | GCB1/IO44PDB2V0 |
| 136 | IO51NSB1V0 | GCC0/IO43NDB2V0 |
| 137 | VCCIB1 | GCC1/IO43PDB2V0 |
| 138 | GND | IO42NDB2V0 |
| 139 | VCC | IO42PDB2V0 |
| 140 | IO50NDB1V0 | IO41NDB2V0 |
| 141 | IO50PDB1V0 | GCC2/IO41PDB2V0 |
| 142 | GCA0/IO49NDB1V0 | VCCIB2 |
| 143 | GCA1/IO49PDB1V0 | GND |
| 144 | GCB0/IO48NDB1V0 | VCC |
| 145 | GCB1/IO48PDB1V0 | IO40NDB2V0 |
| 146 | GCC0/IO47NDB1V0 | GCB2/IO40PDB2V0 |

FG256



Note

For Package Manufacturing and Environmental information, visit the Resource Center at <http://www.microsemi.com/soc/products/solutions/package/default.aspx>.

| FG256 | | | | |
|------------|-----------------|-----------------|-----------------|------------------|
| Pin Number | AFS090 Function | AFS250 Function | AFS600 Function | AFS1500 Function |
| C7 | IO09RSB0V0 | IO12RSB0V0 | IO06NDB0V0 | IO09NDB0V1 |
| C8 | IO14RSB0V0 | IO22RSB0V0 | IO16PDB1V0 | IO23PDB1V0 |
| C9 | IO15RSB0V0 | IO23RSB0V0 | IO16NDB1V0 | IO23NDB1V0 |
| C10 | IO22RSB0V0 | IO30RSB0V0 | IO25NDB1V1 | IO31NDB1V1 |
| C11 | IO20RSB0V0 | IO31RSB0V0 | IO25PDB1V1 | IO31PDB1V1 |
| C12 | VCCIB0 | VCCIB0 | VCCIB1 | VCCIB1 |
| C13 | GBB1/IO28RSB0V0 | GBC1/IO35RSB0V0 | GBC1/IO26PPB1V1 | GBC1/IO40PPB1V2 |
| C14 | VCCIB1 | VCCIB1 | VCCIB2 | VCCIB2 |
| C15 | GND | GND | GND | GND |
| C16 | VCCIB1 | VCCIB1 | VCCIB2 | VCCIB2 |
| D1 | GFC2/IO50NPB3V0 | IO75NDB3V0 | IO84NDB4V0 | IO124NDB4V0 |
| D2 | GFA2/IO51NDB3V0 | GAB2/IO75PDB3V0 | GAB2/IO84PDB4V0 | GAB2/IO124PDB4V0 |
| D3 | GAC2/IO51PDB3V0 | IO76NDB3V0 | IO85NDB4V0 | IO125NDB4V0 |
| D4 | GAA2/IO52PDB3V0 | GAA2/IO76PDB3V0 | GAA2/IO85PDB4V0 | GAA2/IO125PDB4V0 |
| D5 | GAB2/IO52NDB3V0 | GAB0/IO02RSB0V0 | GAB0/IO02NPB0V0 | GAB0/IO02NPB0V0 |
| D6 | GAC0/IO04RSB0V0 | GAC0/IO04RSB0V0 | GAC0/IO03NDB0V0 | GAC0/IO03NDB0V0 |
| D7 | IO08RSB0V0 | IO13RSB0V0 | IO06PDB0V0 | IO09PDB0V1 |
| D8 | NC | IO20RSB0V0 | IO14NDB0V1 | IO15NDB0V2 |
| D9 | NC | IO21RSB0V0 | IO14PDB0V1 | IO15PDB0V2 |
| D10 | IO21RSB0V0 | IO28RSB0V0 | IO23PDB1V1 | IO37PDB1V2 |
| D11 | IO23RSB0V0 | GBB0/IO36RSB0V0 | GBB0/IO27NDB1V1 | GBB0/IO41NDB1V2 |
| D12 | NC | NC | VCCIB1 | VCCIB1 |
| D13 | GBA2/IO31PDB1V0 | GBA2/IO40PDB1V0 | GBA2/IO30PDB2V0 | GBA2/IO44PDB2V0 |
| D14 | GBB2/IO31NDB1V0 | IO40NDB1V0 | IO30NDB2V0 | IO44NDB2V0 |
| D15 | GBC2/IO32PDB1V0 | GBB2/IO41PDB1V0 | GBB2/IO31PDB2V0 | GBB2/IO45PDB2V0 |
| D16 | GCA2/IO32NDB1V0 | IO41NDB1V0 | IO31NDB2V0 | IO45NDB2V0 |
| E1 | GND | GND | GND | GND |
| E2 | GFB0/IO48NPB3V0 | IO73NDB3V0 | IO81NDB4V0 | IO118NDB4V0 |
| E3 | GFB2/IO50PPB3V0 | IO73PDB3V0 | IO81PDB4V0 | IO118PDB4V0 |
| E4 | VCCIB3 | VCCIB3 | VCCIB4 | VCCIB4 |
| E5 | NC | IO74NPB3V0 | IO83NPB4V0 | IO123NPB4V0 |
| E6 | NC | IO08RSB0V0 | IO04NPB0V0 | IO05NPB0V1 |
| E7 | GND | GND | GND | GND |
| E8 | NC | IO18RSB0V0 | IO08PDB0V1 | IO11PDB0V1 |
| E9 | NC | NC | IO20NDB1V0 | IO27NDB1V1 |
| E10 | GND | GND | GND | GND |
| E11 | IO24RSB0V0 | GBB1/IO37RSB0V0 | GBB1/IO27PDB1V1 | GBB1/IO41PDB1V2 |
| E12 | NC | IO50PPB1V0 | IO33PSB2V0 | IO48PSB2V0 |

| FG256 | | | | |
|-------------------|------------------------|------------------------|------------------------|-------------------------|
| Pin Number | AFS090 Function | AFS250 Function | AFS600 Function | AFS1500 Function |
| R5 | AV0 | AV0 | AV2 | AV2 |
| R6 | AT0 | AT0 | AT2 | AT2 |
| R7 | AV1 | AV1 | AV3 | AV3 |
| R8 | AT3 | AT3 | AT5 | AT5 |
| R9 | AV4 | AV4 | AV6 | AV6 |
| R10 | NC | AT5 | AT7 | AT7 |
| R11 | NC | AV5 | AV7 | AV7 |
| R12 | NC | NC | AT9 | AT9 |
| R13 | NC | NC | AG9 | AG9 |
| R14 | NC | NC | AC9 | AC9 |
| R15 | PUB | PUB | PUB | PUB |
| R16 | VCCIB1 | VCCIB1 | VCCIB2 | VCCIB2 |
| T1 | GND | GND | GND | GND |
| T2 | NCAP | NCAP | NCAP | NCAP |
| T3 | VCC33N | VCC33N | VCC33N | VCC33N |
| T4 | NC | NC | ATR TN0 | ATR TN0 |
| T5 | AT1 | AT1 | AT3 | AT3 |
| T6 | ATR TN0 | ATR TN0 | ATR TN1 | ATR TN1 |
| T7 | AT2 | AT2 | AT4 | AT4 |
| T8 | ATR TN1 | ATR TN1 | ATR TN2 | ATR TN2 |
| T9 | AT4 | AT4 | AT6 | AT6 |
| T10 | ATR TN2 | ATR TN2 | ATR TN3 | ATR TN3 |
| T11 | NC | NC | AT8 | AT8 |
| T12 | NC | NC | ATR TN4 | ATR TN4 |
| T13 | G NDA | G NDA | G NDA | G NDA |
| T14 | VCC33A | VCC33A | VCC33A | VCC33A |
| T15 | VAREF | VAREF | VAREF | VAREF |
| T16 | GND | GND | GND | GND |

| Revision | Changes | Page |
|-----------------------------|---|-------|
| Advance v1.5 (continued) | This bullet was added to the " Integrated A/D Converter (ADC) and Analog I/O " section: ADC Accuracy is Better than 1% | I |
| | In the " Integrated Analog Blocks and Analog I/Os " section, ± 4 LSB was changed to 0.72. The following sentence was deleted: The input range for voltage signals is from -12 V to $+12$ V with full-scale output values from 0.125 V to 16 V. In addition, 2°C was changed to 3°C : "One analog input in each quad can be connected to an external temperature monitor diode and achieves detection accuracy of $\pm 3^\circ\text{C}$." The following sentence was deleted: The input range for voltage signals is from -12 V to $+12$ V with full-scale output values from 0.125 V to 16 V. | 1-4 |
| | The title of the datasheet changed from Actel Programmable System Chips to Actel Fusion Mixed Signal FPGAs. In addition, all instances of programmable system chip were changed to mixed signal FPGA. | N/A |
| Advance v1.4 (July 2008) | In Table 3-8 • Quiescent Supply Current Characteristics (IDDQ)1 , footnote references were updated for I_{DC2} and I_{DC3} . Footnote 3 and 4 were updated and footnote 5 is new. | 3-11 |
| Advance v1.3 (July 2008) | The " ADC Description " section was significantly updated. Please review carefully. | 2-102 |
| Advance v1.2 (May 2008) | Table 2-25 • Flash Memory Block Timing was significantly updated. | 2-55 |
| | The " V_{AREF} Analog Reference Voltage " pin description section was significantly update. Please review it carefully. | 2-226 |
| | Table 2-45 • ADC Interface Timing was significantly updated. | 2-110 |
| | Table 2-56 • Direct Analog Input Switch Control Truth Table—AV (x = 0), AC (x = 1), and AT (x = 3) was significantly updated. | 2-131 |
| | The following sentence was deleted from the " Voltage Monitor " section: The Analog Quad inputs are tolerant up to 12 V + 10%. | 2-86 |
| | The " 180-Pin QFN " figure was updated. D1 to D4 are new and the figure was changed to bottom view. The note below the figure is new. | 3-3 |
| Advance v1.1 (May 2008) | The following text was incorrect and therefore deleted: VCC33A Analog Power Filter Analog power pin for the analog power supply low-pass filter. An external 100 pF capacitor should be connected between this pin and ground. There is still a description of V_{CC33A} on page 2-224 . | 2-204 |